

Wear properties under dry sliding of Lu- α sialons with in situ reinforced microstructures

Mark I. Jones^{a,*}, Hideki Hyuga^b, Kiyoshi Hirao^a, Yukihiro Yamauchi^a

^a Synergy Materials Research Center, AIST, 2268-1 Shimo-shidami, Nagoya 463-8687, Japan

^b Fine Ceramics Research Association, 2268-1 Shimo-shidami, Nagoya 463-8687, Japan

Received 8 September 2003; received in revised form 20 November 2003; accepted 28 November 2003

Available online 15 April 2004

Abstract

In situ reinforced microstructures in Lu- α sialons have been developed by sintering compositions which resulted in the presence of an extended liquid phase, and which forms a secondary crystalline grain boundary phase on cooling. The wear properties of these materials have been assessed under dry sliding conditions through block on ring wear tests under different loads, and compared with the wear properties of an equiaxed Lu- α sialon, which had good wear resistance under low loads but a high wear rate under higher loads. The presence of the elongated grain microstructure resulted in improvements in mechanical properties and a reduction in the high load specific wear rate of about 1 order of magnitude. Under low load wear tests, samples sintered with Lu₂SiO₅ as the additional liquid former resulted in an increase in wear rate due to extensive removal of the silicate grain boundary phase. However, samples in which the liquid formation was achieved through additions of Lu₂O₃ only, in addition to reducing the high load wear rate, maintained the good low load wear resistance seen for the equiaxed material.

© 2004 Elsevier Ltd. All rights reserved.

Keywords: Sialons; Microstructure; Wear resistance; Testing

1. Introduction

The two polymorphs of silicon nitride, α and β , have distinctly different microstructures. Anisotropic growth rates in the β phase result in the formation of an elongated grain microstructure, whereas the α phase always exists with an equiaxed microstructure. These distinct microstructures result in significantly different mechanical properties, with the α phase being harder than the β phase, but the resistance to crack propagation through crack bridging effects in the latter results in higher fracture toughness. Incorporation of Al and O into a Si₃N₄ matrix results in the family of ceramics known as SiAlONs, of which the two most commonly studied phases are again the α and β phases, isostructural with α and β Si₃N₄, respectively. Although sialons are based on the Si₃N₄ structure there are several significant differences between the two. Firstly, whereas a polymorphic transformation of α to β occurs on sintering in Si₃N₄, in sialons both phases are compatible. This means that the overall phase composition is determined by the composition of the starting

powder mixtures, and there is a greater potential for microstructural control. Secondly, in silicon nitrides, the oxides commonly used to aid sintering, typically Al₂O₃ and a rare earth oxide, RE₂O₃, result in the presence of an intergranular glassy phase, which has a significant effect on the mechanical properties.¹ In sialons the incorporation of the Al and O into the Si₃N₄ structure, results in the possibility of producing dense materials with reduced amount of grain boundary phase. This is particularly true for the α phase, which is given by the formula RE_xSi_{12-(m+n)}Al_(m+n)O_nN_{16-n}. In this formula the charge discrepancy arising from the substitution of m (Si–N) bonds by (Al–N) and n (Si–N) being replaced by (Al–O) is compensated for by the incorporation of the rare earth ion RE^{p+}.² Finally, although the α Si₃N₄ phase has only ever been observed to possess an equiaxed grain morphology, it has been shown that the sialon α phase can develop an elongated grain morphology similar to the β phases and can also lead to improvements in fracture toughness.³ The development of such microstructures is most commonly achieved through seeding of the starting powders,⁴ using starting compositions which result in extended transient liquid formation⁵ and/or rapid sintering techniques such as spark plasma sintering, SPS.⁶

* Corresponding author.

E-mail address: mark.jones@aist.go.jp (M.I. Jones).

There are several wear mechanisms involved in the wear of silicon nitride based materials depending on the sliding conditions. Under low loads and relatively low temperatures one of the dominant wear mechanisms is tribochemical wear. Tribochemical wear occurs when reactions between the sliding surface and water vapor in the air, stimulated by friction, results in the formation of an amorphous $\text{Si}(\text{OH})_4$ layer, and wear is determined by the rate of formation and removal of this film.⁷ Under higher loads, the dominant wear mechanism is one of mechanical wear, occurring by the propagation of cracks along grain boundaries, and resulting in micro fracture within the material.⁸ Such intergranular cracking can lead to the “pulling out” or “dropping” of grains from the material surface,⁹ and generally results in higher wear rates than those associated with tribochemical type wear.

In earlier work on the wear properties of Y stabilized α/β composite sialons it was shown that under high loads, where microcracking and grain dropping was dominant, the higher fracture toughness of composites containing a high β content (elongated grain morphology) gave better resistance to crack propagation and lower wear volumes than single phase, equiaxed, α sialons.¹⁰ However under low loads where tribochemical wear was thought to be predominant, the single phase α materials had better wear resistance, attributed to reduced amount of intergranular glassy phase and improved thermal stability. Indeed in a later paper it was shown that under these conditions the low load wear resistance could be improved by substitution of the Y stabilizing cation by one of a more refractory nature.¹¹ These Lu-stabilized α -sialons showed wear volumes an order of magnitude lower than the Y α sialon under low loads, but the low fracture toughness associated with the equiaxed microstructure again resulted in high wear under more severe testing conditions. Producing α/β composites of these materials with elongated β grains resulted in improved high load wear resistance but, as with the Y stabilized composites, the low load wear resistance was inferior when compared to the single phase α materials. These results indicated that when the α/β composite approach was employed to control the microstructure and mechanical properties, a trade off type relationship between materials suitable for different wear environments was observed. In the present work we report an attempt to combine the chemical stability suitable for tribochemical type wear with the microstructural features suitable for high load wear resistance by producing in situ reinforced Lu-sialon materials where the in situ reinforcement by elongated grains has been achieved in the α phase. The effect of such microstructures on the mechanical and wear properties is discussed.

2. Experimental

In α sialon materials where the stabilizing rare earth cation has a 3^+ valency, the overall composition is given by the formula $\text{RE}_{m/3}\text{Si}_{12-(m+n)}\text{Al}_{(m+n)}\text{O}_n\text{N}_{16-n}$. The

target composition based on this formula was one where $m = n = 1.1$, which has been shown previously to result in an equiaxed, single phase Lu- α sialon. In order to develop the elongated grain microstructure, an additional liquid phase was promoted by the addition of either Lu_2O_3 or Lu monosilicate, Lu_2SiO_5 . In both cases the total addition was 5% by weight. When calculating the compositions the oxygen content of the nitride powders was taken into consideration. The samples were produced by mixing appropriate amounts of α - Si_3N_4 (E-10 grade, Ube Industries, Ltd., Japan), Al_2O_3 (AKP-50, Sumitomo Chemical Co., Ltd., Japan), AlN (F grade, Tokuyama Co., Japan), SiO_2 (99.9% Kojundo Chemical Laboratory Co., Ltd, Japan) and Lu_2O_3 (99.9%, Shin-Etsu Chemical Co., Ltd., Japan) in methanol using a Si_3N_4 pot and Si_3N_4 balls. The slurry was dried, and then passed through 125 mesh. Sintering was carried out by hot pressing the sieved powders in a boron nitride coated graphite die at 1950°C for 2 h with an applied pressure of 40 MPa in a 0.9 MPa N_2 atmosphere. Phase identification was carried out by X-ray diffractometry of powder samples crushed following sintering, and the fracture surfaces of the samples following sintering were observed by scanning electron microscopy, SEM (JSM-6340F, JEOL Ltd., Japan). For mechanical property measurements, test bars with dimensions of $3\text{ mm} \times 4\text{ mm} \times 40\text{ mm}$ were machined from the sintered specimens and polished on the tensile face down to $0.5\text{ }\mu\text{m}$ diamond slurry. Samples for Block-on-Ring tests were machined in the same way to a size of $3\text{ mm} \times 4\text{ mm} \times 1.5\text{ mm}$ thickness. Strength measurements were carried out by four-point bending with inner and outer spans of 10 and 30 mm, respectively, and a crosshead speed of 0.5 mm min^{-1} . Vickers hardness was determined under a load of 98 N, and fracture toughness (K_{IC}) was determined by the indentation-fracture (IF) method under the same load. In all experiments, the samples were tested on the face normal to the hot pressing direction, and the results are given as the average of five tests. Block-on-Ring tests were carried out under non-lubricated conditions using the equipment described in a previous paper.¹⁰ The sialon samples were employed as the blocks and were located in a holder above the ring, which was a commercially available silicon nitride material (SN235P, Kyocera, Japan) of 35 mm diameter. The surface roughness of both the Si_3N_4 ring and the sialon specimens were prepared under R_z $0.1\text{ }\mu\text{m}$. Temperature and humidity were kept constant at $25 \pm 3^\circ\text{C}$, $25 \pm 2\%$ RH. Sliding speed and distance were kept constant at 0.15 m s^{-1} and 75 m, respectively, and tests were conducted with normal loads varying from 5 to 90 N. Following wear tests, the worn area of the blocks was measured at nine equidistant points (spacing 0.3 mm) in the direction parallel to the sliding direction by a contact type roughness tester (SV-624, Mitutoyo, Japan) and the wear volume was calculated by integration of the sectional worn area. Specific wear rates were calculated by dividing the worn volume by the product of load and sliding distance. Worn surfaces were observed by SEM.

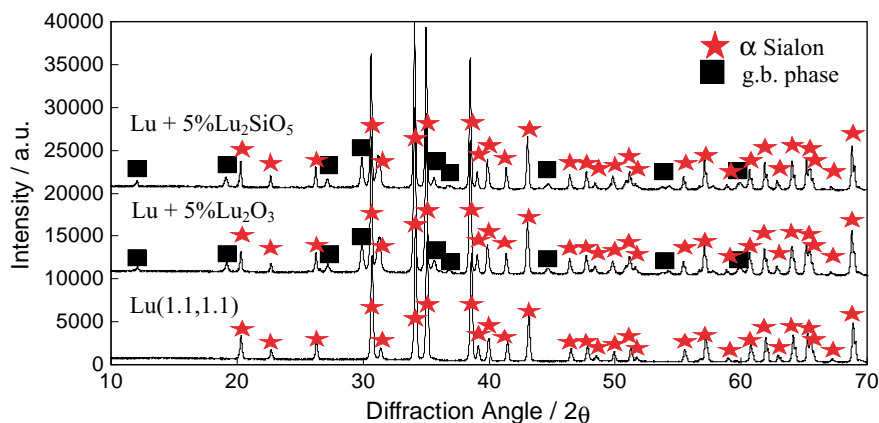


Fig. 1. XRD spectra of the sintered Lu sialon materials. Lu (1.1,1.1) was single phase α sialon. The two materials sintered in the presence of extra liquid showed an additional secondary crystalline phase thought to be produced by crystallisation of the grain boundary phase. This was the same phase for both compositions.

3. Results

For the sample sintered with no additional liquid the starting composition ($m = n = 1.1$) was one in which theoretically all of the transient liquid phase present during sintering, resulting from the addition of the oxides, could enter into the silicon nitride structure and form single phase α sialon, with little or no grain boundary phase. However, in practice some residual boundary phase is often observed at triple junctions. XRD spectra of crushed samples following sintering are shown in Fig. 1. For this sample only single phase α sialon was indeed observed. For the two materials sintered in the presence of an additional liquid, a second crystalline phase was detected and is thought to be grain boundary phase that crystallized on cooling.

Fracture surfaces of the samples following bending tests are shown in Fig. 2 and indicate the general microstructural features. The Lu (1.1,1.1) sample had an equiaxed microstructure with grain size of between 1 and 2 μm , whilst the presence of the liquid phase in the other two samples promoted grain growth. SEM images of polished surfaces of the two samples with elongated grains are shown in Fig. 3 where the grain boundary phase can be observed as high contrast. From this figure it can be seen that the sample sintered in the presence of 5% Lu_2O_3 possessed a coarser microstructure than that of the 5% Lu_2SiO_5 sample. The former sample contained grains around 10 μm in length and thickness up to around 2 μm . In the latter sample grains of similar length were observed but with larger aspect ratio due to the grain thickness typically being less than 1 μm . The effect of the microstructural development on the room temperature mechanical properties is shown in Table 1. With the introduction of the extra liquid and the development of an elongated grain microstructure, there was a very slight decrease in hardness for both of the Lu stabilized materials, but both the bending strength and the fracture toughness measured by indentation fracture was increased.

The specific wear rates of the samples following wear tests at loads of both 5 and 90 N are shown in Fig. 4. For the equiaxed sample a low specific wear rate of $3.7 \times 10^{-7} \text{ mm}^3 \text{ N}^{-1} \text{ m}^{-1}$ was observed under low loads, but under the higher load conditions the wear rate showed a high value of $6.9 \times 10^{-5} \text{ mm}^3 \text{ N}^{-1} \text{ m}^{-1}$. The effect of the additional liquid phase sintered samples on the high load wear rate is seen in Fig. 4, where the specific wear rate was reduced almost one order of magnitude for the 5% Lu_2O_3 and 5% Lu_2SiO_5 samples, respectively. Images of the worn surfaces of these materials are shown in Fig. 5. Whereas the surface of the equiaxed material was essentially free from debris as a result of the intergranular fracture and grain dropping which allowed immediate removal of the grains from the contact area,¹¹ the surfaces of the elongated samples tended to be covered with large amounts of crushed debris as a result of a more gradual wear process. In areas where this debris had been removed microstructural features could be observed as shown in the figure, but such widespread grain dropping as seen for the equiaxed material was not observed.

Compared to the equiaxed sample with no additional liquid phase, the low load specific wear rate of the sample sintered with the rare earth monosilicate addition showed a large increase ($4 \times 10^{-6} \text{ mm}^3 \text{ N}^{-1} \text{ m}^{-1}$). The sample sintered with only additional Lu_2O_3 maintained the low wear rate observed for the equiaxed material

Table 1
Mechanical properties of the equiaxed and elongated Lu- α sialons

Sample	Hardness (GPa)	Bending strength (MPa)	Indentation toughness ($\text{MPa m}^{1/2}$)
Lu- α sialon	19.27 ± 0.76	391 ± 74	2.6 ± 0.11
Lu + 5% Lu_2O_3	18.88 ± 0.63	442 ± 59	4.4 ± 0.11
Lu + 5% Lu_2SiO_5	18.92 ± 0.64	586 ± 40	4.4 ± 0.18

Errors are given as standard deviation.

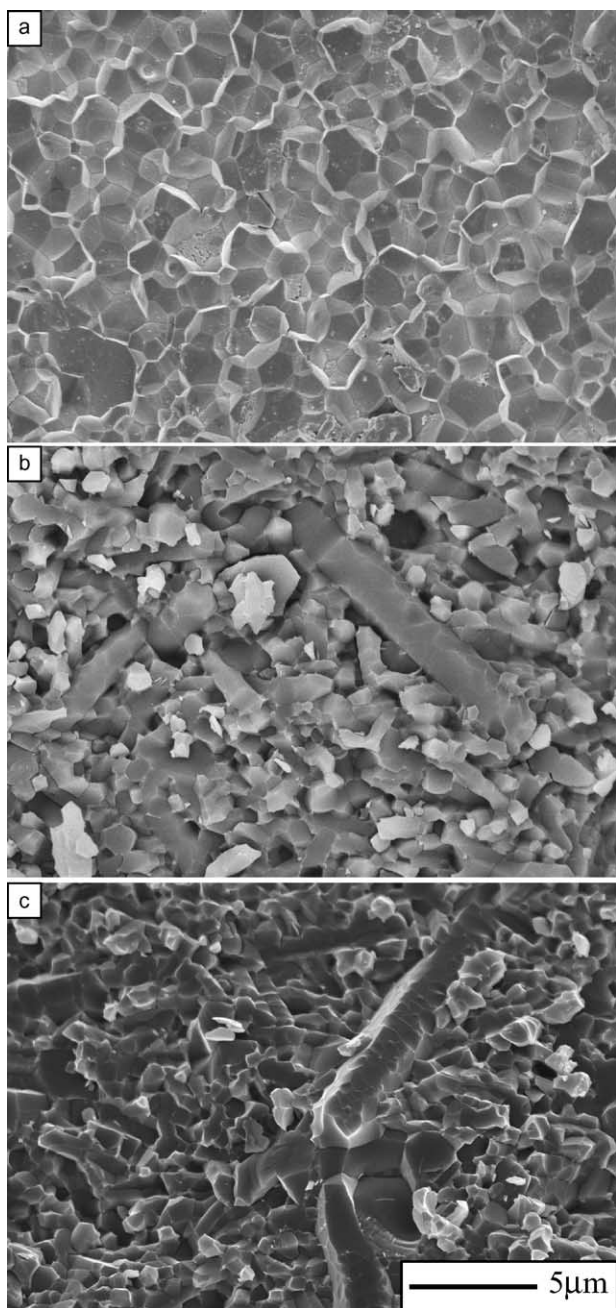


Fig. 2. Fracture surfaces of (a) Lu equiaxed α sialon, (b) Lu + 5% Lu_2O_3 and (c) Lu + 5% Lu_2SiO_5 .

($5 \times 10^{-7} \text{ mm}^3 \text{ N}^{-1} \text{ m}^{-1}$). SEM images of the worn surfaces of these samples under low loads are shown in Fig. 6. In both cases grain boundary removal could be observed. In the case of the sample sintered with Lu_2O_3 this removal was limited and tended to be restricted to triple junction areas. On the other hand, in the case of the Lu_2SiO_5 added sample the grain boundary removal was much more extensive and extended from the triple junctions along the grain boundaries.

4. Discussion

XRD analysis showed that a secondary crystalline grain boundary phase was observed for both samples sintered with extra liquid. Since the sub-solidus phase relationships in the Lu–Si–Al–O–N system have not been derived it is difficult to unambiguously identify the phase. The processing and properties of the Lu- α sialon with 5% Lu_2SiO_5 has been described in a recent publication.¹² In that work a Y- α sialon also sintered in the presence of 5 wt.% RE_2SiO_5 showed the same crystalline phase to be present and it was suggested that for the Y-stabilized material it could be indexed as J' phase, an Al containing solid solution based on J phase ($\text{Y}_4\text{Si}_2\text{O}_7\text{N}_2$). The general formula of this phase is given by $\text{Y}_4\text{Si}_{2-x}\text{Al}_x\text{O}_{7+x}\text{N}_{2-x}$ and is formed through solid solution of J phase and YAM ($\text{Y}_4\text{Al}_2\text{O}_9$). It was suggested that the same peak pattern in the case of the Lu- α sialon with 5 wt.% Lu_2SiO_5 , although shifted to slightly higher peak positions, may imply that this phase can also be produced in the Lu–Si–Al–O–N system. Huang and Chen have shown that the J' phase forms in other RE–Si–Al–O–N systems and that its stability increases with decreasing ionic radius of the RE element.¹³ These authors suggested that this phase probably exists for rare earth elements from dysprosium to ytterbium and that the degree of substitution, x , decreases with decreasing ionic radius, which would explain the shift in peak positions. The phase relationships in the Si_3N_4 – SiO_2 – Lu_2O_3 system have been shown to be very similar to those of the Si_3N_4 – SiO_2 – Yb_2O_3 system, including the formation of J phase,¹⁴ and since the ionic radius of Lu is very similar to that of Yb it is not surprising that J' phase may also exist in the Lu–Si–Al–O–N system. The same crystalline phase was also observed for the Lu- α sialon sintered with 5%– Lu_2O_3 and there was no discernible shift in the peak positions between the two Lu- α sialons sintered with additional liquid. The fact that this silicon oxynitride phase was also observed in the sample to which only Lu_2O_3 was added implies that the actual composition of the Lu- α sialons sintered in the presence of additional liquid may actually be shifted somewhat to lower m and n values than the target composition. However, TEM work is required to fully identify and characterize this phase unambiguously.

The development of elongated microstructures in the samples with additional liquid led to improvements in room temperature strength and fracture toughness. This is due to the elongated grains facilitating toughening mechanisms such as crack bridging and crack deflection as is often observed in in situ reinforced silicon nitride ceramics.¹⁵ Hoffmann and Holzer showed that for sialons sintered with different rare earths, the addition of extra liquid resulted in higher fracture toughness due to a more elongated microstructure and a weaker interface between the matrix and the residual glass.¹⁶ The smaller strength increase for the 5% Lu_2O_3 sample compared with that of the 5% Lu_2SiO_5 one is attributed to the coarser microstructure, with the larger grains acting as larger defect sites.

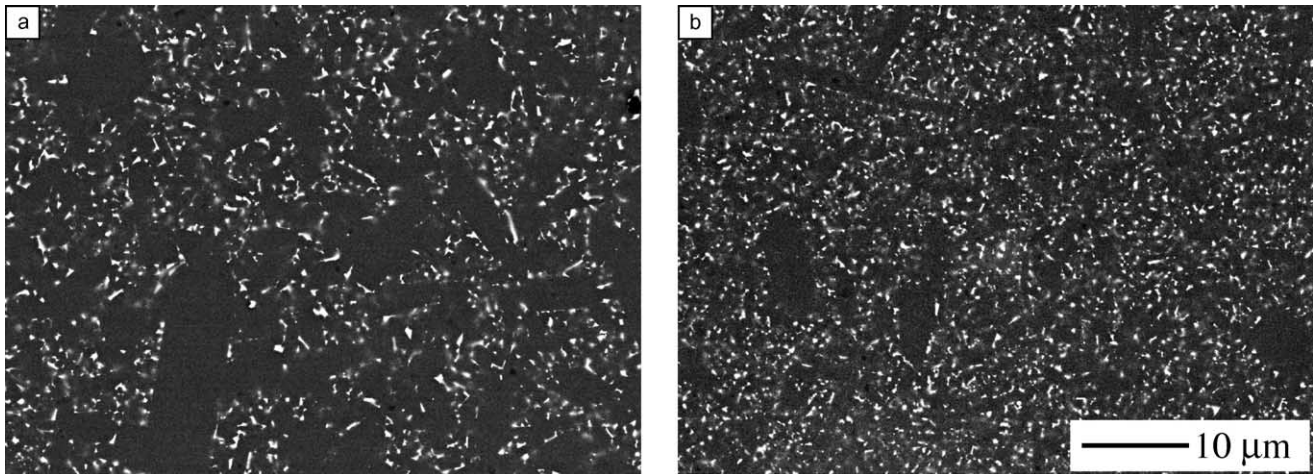


Fig. 3. Polished surfaces of (a) Lu + 5% Lu_2O_3 and (b) Lu + 5% Lu_2SiO_5 . A coarser microstructure was observed in the former. The grain boundary phase can be observed as high contrast in both cases.

The equiaxed α material showed good wear resistance under low loads, but a very high wear rate under higher loads. The differences in wear rate for this material have been explained in a recent paper as being a result of the different wear mechanisms acting under the different conditions.¹¹ In that paper SEM images of worn surfaces showed that under low loads the worn surface was very smooth and traces of grain boundary removal were observed. It is thought that under those conditions tribochemical type wear was dominant, and the grain boundary removal occurred by adhesion of the residual silicate boundary phase with the opposing silicon nitride ring. The high wear resistance of the single phase α material was attributed to low amount of grain boundary phase and the refractory nature of the Lu stabilizing cation. Work on silicon nitride ceramics sintered with different rare earth disilicate additions has shown that rare earths with smaller ionic radius resulted in improved oxidation resistance.¹⁷ The same trend of improved oxidation resistance with decreasing cation

size has also been reported for α sialon ceramics¹⁸ and rare earth silicon oxynitride glasses.¹⁹ Under high load conditions however the wear rate was high and the worn surface showed appearance similar to a fracture surface, with intergranular fracture and removal or pull-out of individual grains. This high wear rate was attributed to the low resistance to microcrack propagation due to the lack of fracture toughness of the equiaxed material. In the current work, the improved mechanical properties in the samples with additional liquid, due to the presence of the elongated microstructures, are thought to be responsible for the improvement in the wear resistance under high loads. The improved fracture strength and toughness of these samples helps to prevent the grain pull-out that was predominant in the equiaxed material. These results show that the improved mechanical properties arising through the formation of the in situ reinforced microstructure in the α phase can be an effective way of improving the wear resistance under high loads, in the same way as producing α/β composites

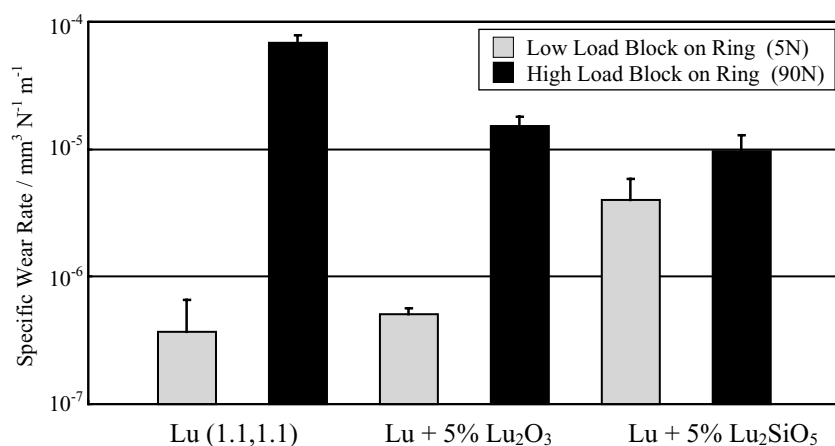


Fig. 4. Specific wear rates of the sintered sialons following block on ring wear tests under normal loads of 5 and 90 N. Error given as standard deviation.

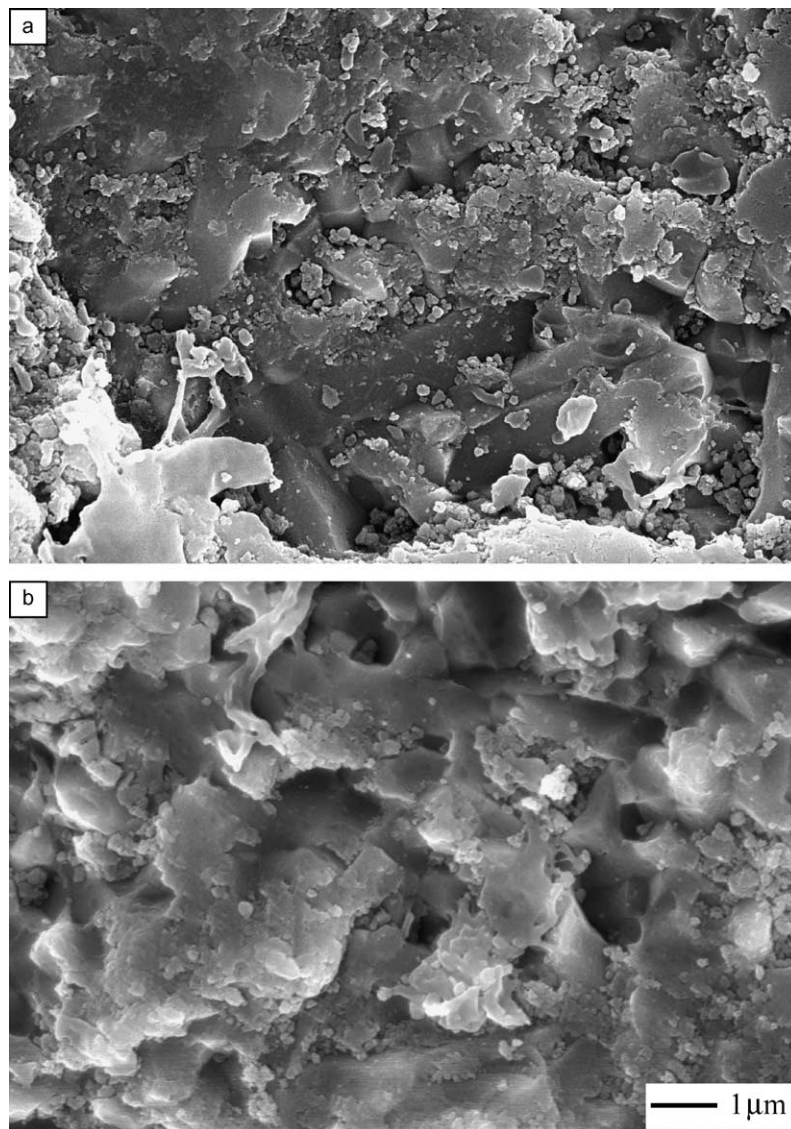


Fig. 5. Surfaces following high load wear tests of the elongated α sialons. (a) Lu + 5% Lu_2O_3 , and (b) Lu + 5% Lu_2SiO_5 samples. Although the wear surfaces show obvious signs of severe type wear, the extensive grain drooping seen for the equiaxed material was not observed.

with elongated β grains was shown to be previously.^{10,11} However, in the previous work, this was at the expense of low load tribochemical wear resistance as a consequence of a higher grain boundary phase content and reduced oxidation resistance. The question that therefore arises is whether or not developing the elongated microstructure in the α phase through the presence of an additional liquid phase can, in addition to improving mechanical properties and high load wear resistance, maintain the good wear resistance observed for the equiaxed material under low load tribochemical wear. The wear rates given in Fig. 4 show that under low loads the wear resistance depended significantly on the nature of the additional liquid used to develop the elongated microstructures. The sample sintered with 5% Lu_2O_3 maintained a low wear rate comparable to that of the equiaxed material, whereas the specific wear

rate of the sample sintered with 5% Lu_2SiO_5 showed a large increase. Much more extensive grain boundary removal was also observed for this sample (Fig. 6) and it is thought that cracks originating from these areas lead to areas of greater material removal and the increased wear rate.

The higher grain boundary removal in the case of the 5% Lu_2SiO_5 sample occurred despite the fact that the crystalline boundary phase was the same as that observed in the 5% Lu_2O_3 one. In both these samples the additional material added to promote the liquid phase was a total of 5% by weight, which gives slightly different volume fractions. This difference is not thought to be responsible for the differences in wear rate since the higher atomic weight of the Lu_2SiO_5 gives a lower volume fraction of additives. However, the volume fraction of SiO_2 in the two samples was significantly

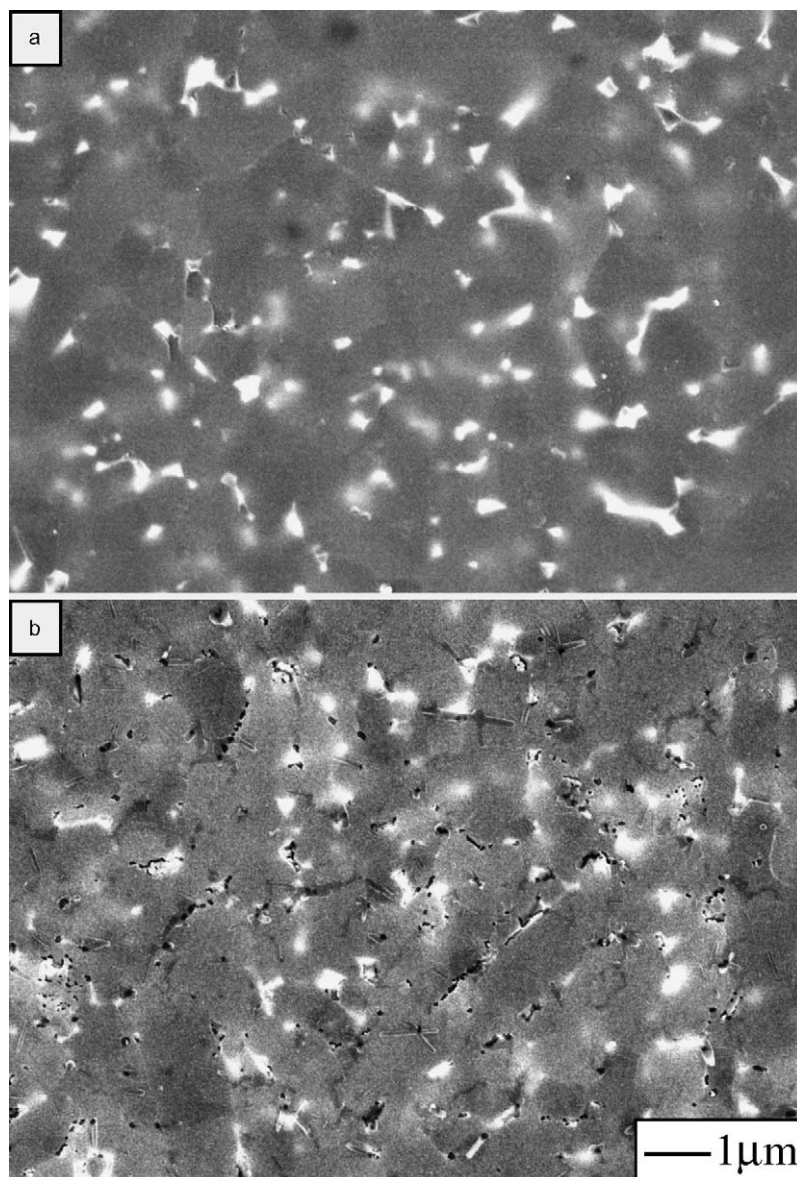


Fig. 6. Worn surfaces of (a) Lu + 5% Lu_2O_3 and (b) Lu + 5% Lu_2SiO_5 samples following low load block on ring wear tests. Much more extensive grain boundary removal was observed in the latter thought to be due to adhesion of the excess SiO_2 with the counter body material.

different. Both samples contained silica present on the surface of the Si_3N_4 starting powder, but this was accounted for in the starting compositions. The sample sintered with the addition of the mono-silicate composition obviously contained additional silica over and above this whilst there was no additional SiO_2 present in the case of the sample sintered with Lu_2O_3 . Calculation shows that the total SiO_2 in the monosilicate addition is around 4 vol.% of the total starting powder composition. Fig. 7 shows EDX analysis from both the grains and grain boundaries of the two samples with extra liquid. The spectra from the grains of the two materials are very similar whereas the spectra from the grain boundaries shows a much lower Lu concentration in the case of the sample with 5% Lu_2SiO_5 sample. Comparing the intensities of

the Lu and Si peaks of these boundary areas therefore gives a higher Si:Lu ratio in the case of the sample with the monosilicate addition, indicating a higher Si content. As described earlier, the oxy-nitride grain boundary crystalline secondary phase observed in the two materials was the same, and since this phase could form in the presence of additional Lu_2O_3 only, there is the possibility that in the Lu_2SiO_5 added sample the additional SiO_2 remains as amorphous silica at the grain boundaries. It is thought that this could be the reason for the more extensive grain boundary removal observed for the 5% Lu_2SiO_5 sample, as during tribochemical type wear it could lead to softening and promote adhesion with the counter body material, leading to the higher wear rate for this sample.

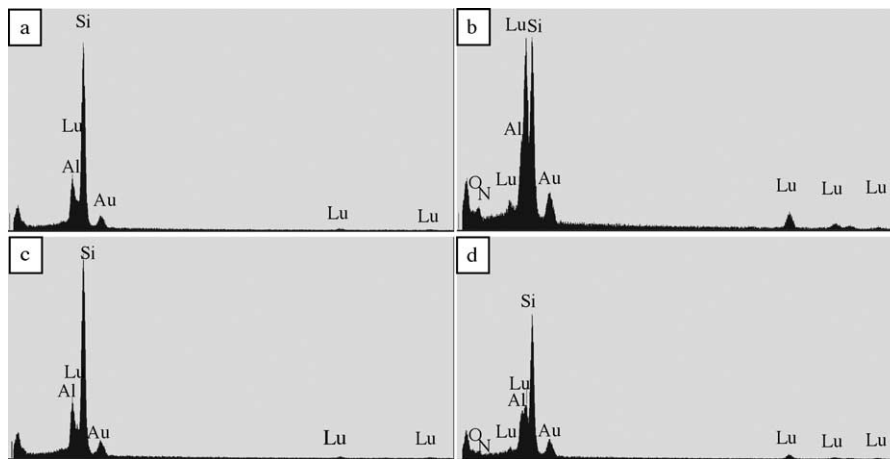


Fig. 7. EDX analysis taken from (a, b) Lu + 5% Lu_2O_3 and (c, d) Lu + 5% Lu_2SiO_5 samples. Analysis of the grains (a and c) showed similar spectra but the grain boundary analysis (b and d) showed a much lower relative concentration of Lu in the case of the sample sintered with the rare earth monosilicate.

5. Conclusions

In situ reinforced Lu- α sialons have been produced through hot pressing in the presence of 5 wt.% of either Lu_2O_3 or Lu_2SiO_5 to promote extended liquid formation during sintering, and the wear properties under both low and high loads has been assessed by block on ring wear tests under dry conditions. Under high load wear, the improved mechanical properties of these samples produced by the development of an elongated grain microstructure resulted in lower specific wear rates when compared with an equiaxed Lu- α sialon. Under low load wear conditions the equiaxed sample showed a low specific wear rate due to limited amount of grain boundary phase, but the wear resistance of the elongated samples was dependent on the nature of the additional liquid phase. Samples sintered with both Lu_2O_3 and Lu_2SiO_5 showed the same crystalline grain boundary phase, but in the case of the Lu_2SiO_5 a much higher wear rate. During low load, tribochemical type wear this sample showed extensive grain boundary removal thought to be due to adhesion between the additional SiO_2 in this sample and the silicate boundary phase of the opposing counter material, and grain boundary cracking resulting from these areas of grain boundary removal resulted in higher wear rates for this sample. In contrast, the α sialon sample sintered with 5% Lu_2O_3 , in addition to reducing the high load wear rate, maintained the low load wear resistance observed for the equiaxed α material.

References

1. Sun, E. Y., Becher, P. F., Plucknett, K. P., Hsueh, C.-H., Alexander, K. B., Waters, S. B. *et al.*, Microstructural design of silicon nitride with improved fracture toughness. II. Effects of yttria and alumina additives. *J. Am. Ceram. Soc.* 1999, **81**(11), 2049–2831.
2. Izhevskiy, V. A., Genova, L. A., Bressiani, J. C. and Aldinger, F., Progress in SiAlON ceramics. *J. Eur. Ceram. Soc.* 2000, **20**, 2275–2295.
3. Chen, I.-W. and Rosenflanz, A., A tough SiAlON ceramic based on α - Si_3N_4 with a whisker-like microstructure. *Nature* 1997, **389**, 701–704.
4. Kim, J., Rosenflanz, A. and Chen, I.-W., Microstructure control of in situ toughened α -SiAlON ceramics. *J. Am. Ceram. Soc.* 2000, **12**(7), 1819–1821.
5. Shen, Z., Nordberg, L. O., Nygren, M. and Ekstrom, T., α -Sialon grains with high aspect ratio-utopia or reality? In *Engineering Ceramics '96: Higher Reliability Through Processing*. Kluwer Academic Publishers, Dordrecht, The Netherlands, 1997, pp. 169–176.
6. Shen, Z., Zhao, Z., Peng, H. and Nygren, M., Formation of tough interlocking microstructures in silicon nitride ceramics by dynamic ripening. *Nature* 2002, **417**, 266–269.
7. Dong, X. and Jahanmir, S., Wear transition diagram for silicon nitride. *Wear* 1993, **165**, 169–180.
8. Wang, Y. and Hsu, S. M., Wear and wear transition mechanisms of ceramics. *Wear* 1996, **195**, 112–122.
9. Park, D.-S., Han, B.-D., Lim, D.-S. and Yeo, I.-W., A study on wear and erosion of sialon- Si_3N_4 whisker ceramic composites. *Wear* 1997, **203/204**, 284–290.
10. Jones, M. I., Hirao, K., Hyuga, H., Yamauchi, Y. and Kanzaki, S., Wear properties of Y- α/β composite sialon ceramics. *J. Eur. Ceram. Soc.* 2003, **23**, 1743–1750.
11. Jones, M. I., Hyuga, H., Hirao, K. and Yamauchi, Y., Wear behaviour of single phase and composite sialon ceramics stabilized with Y_2O_3 and Lu_2O_3 . *J. Eur. Ceram. Soc.*, in press.
12. Jones, M. I., Hyuga, H., Hirao, K. and Yamauchi, Y., Processing and properties of in-situ reinforced α sialons stabilized with Y_2O_3 and Lu_2O_3 . *J. Am. Ceram. Soc.*, in press.
13. Huang, Z.-K. and Chen, I.-W., Rare-earth melilite solution and its phase relations with neighboring phases. *J. Am. Ceram. Soc.* 1996, **79**(8), 2091–2097.
14. Hirotsaki, N., Yamamoto, Y., Nishimura, T., Mitomo, M., Takahashi, J., Yamane, H. *et al.*, Phase relationships in the Si_3N_4 - SiO_2 - Lu_2O_3 system. *J. Am. Ceram. Soc.* 2002, **85**(11), 2861–2863.
15. Becher, P. F., Sun, E. Y., Plucknett, K. P., Alexander, K. B., Hsueh, C. H., Lin, H. T. *et al.*, Microstructural design of silicon nitride with improved fracture toughness. 1. Effects of grain shape and size. *J. Am. Ceram. Soc.* 1998, **81**(11), 2821–2830.

16. Hoffmann, M. J. and Holzer, S., Processing and microstructural evolution of rare earth containing sialons. *Key. Eng. Mater.* 2003, **237**, 141–148.
17. Cinibulk, M. K., Thomas, G. and Johnson, S. M., Oxidation behavior of rare-earth disilicate-silicon nitride ceramics. *J. Am. Ceram. Soc.* 1992, **75**(8), 2044–2049.
18. Nakayama, S., Shiranita, A., Ayuzawa, N. and Sakamoto, M., Oxidation behavior of RE- α -sialon ceramics (RE = Nd, Sm, Gd, Dy, Y, Ho, Er, Yb). *J. Ceram. Soc. Jpn.* 1993, **101**(10), 1184–1186.
19. Murakami, Y. and Yamamoto, H., Properties of oxynitride glasses in the Ln–Si–Al–O–N systems (Ln = rare earth). *J. Ceram. Soc. Jpn.* 1994, **102**(3), 231–236.